OPTICALLY PUMPED MID-IR VIBRATIONAL HYDROGEN CHLORIDE LASER

Harold C. Miller, John McCord, and Gordon D. Hager
Air Force Research Laboratory
Lasers and Imaging Directorate
Kirtland AFB, NM 87117-5776

and

Steven J. Davis, William J. Kessler, and David B. Oakes
Physical Sciences Inc.
20 New England Business Center
Andover, MA 01810-1077

Reprinted with permission from *Journal of Applied Physics*, **84**(7), pp. 3467-3473, October 1, 1998.

Report Documentation Page

Form Approved
OMB No. 0704-0188

1. REPORT DATE	2. REPORT TYPE	3. DATES COVERED
1998		**00-00-1998 to 00-00-1998**

4. TITLE AND SUBTITLE	5a. CONTRACT NUMBER
Optically Pumped Mid-IR Vibrational Hydrogen Chloride Laser	5b. GRANT NUMBER
	5c. PROGRAM ELEMENT NUMBER
6. AUTHOR(S)	5d. PROJECT NUMBER
	5e. TASK NUMBER
	5f. WORK UNIT NUMBER
7. PERFORMING ORGANIZATION NAME(S) AND ADDRESS(ES) **Air Force Research Laboratory,Lasers and Imaging Directorate,Kirtland AFB,NM,87117-5776**	8. PERFORMING ORGANIZATION REPORT NUMBER
9. SPONSORING/MONITORING AGENCY NAME(S) AND ADDRESS(ES)	10. SPONSOR/MONITOR'S ACRONYM(S)
	11. SPONSOR/MONITOR'S REPORT NUMBER(S)

12. DISTRIBUTION/AVAILABILITY STATEMENT
Approved for public release; distribution unlimited

13. SUPPLEMENTARY NOTES

14. ABSTRACT
see report

15. SUBJECT TERMS

16. SECURITY CLASSIFICATION OF:			17. LIMITATION OF ABSTRACT	18. NUMBER OF PAGES	19a. NAME OF RESPONSIBLE PERSON
a. REPORT **unclassified**	b. ABSTRACT **unclassified**	c. THIS PAGE **unclassified**		**29**	

OPTICALLY PUMPED MID-IR VIBRATIONAL HYDROGEN CHLORIDE LASER

Harold C. Miller, John McCord, and Gordon D. Hager

Air Force Research Laboratory

Lasers and Imaging Directorate

Kirtland AFB, NM 87117-5776

and

Steven J. Davis, William J. Kessler, and David B. Oakes

Physical Sciences Inc.

20 New England Business Center

Andover, MA 01810-1077

Abstract

The results of an experimental investigation of an optically pumped vibrational laser in HCl are reported. Two different excitation sources were used: a Nd:YAG laser pumped optical parametric oscillator and a Raman shifted alexandrite laser. Overtone pumping on the (2,0) and (3,0) bands was employed to produce laser oscillation on the (3,2) and (2,1) bands near 3.8 microns. We also developed a model for the optically pumped laser and compare predictions of the model to the observed behavior of the laser. The photon efficiency of the HCl laser was found to be approximately 60%, consistent with model predictions and with previous optically pumped hydrogen halide lasers.

I. Introduction

The study of optically pumped lasers has been a fruitful area of research for many years.[1-9] Numerous atomic and molecular species have been studied using optical excitation techniques. Since many of the previous studies used visible wavelength excitation sources, a majority of the optically pumped lasers operated on electronic transitions.

The hydrogen halide molecules are well known laser species via chemical excitation. For example, the HF laser (2.7 μm) derives its energy from the reaction of $F + H_2$ that forms vibrationally inverted HF. The early successes of these chemical lasers led to detailed studies of the radiative dynamics and kinetics of this class of molecules. Consequently, there is a fairly extensive database for the hydrogen halide species.[10-17]

Optical excitation resulting in laser oscillation in selected hydrogen halide molecules has also been the subject of several studies. For example, Skribanowitz and co-workers[18-20] reported observation of laser oscillation on several rovibrational lines in HF following pumping on the (1,0) band using a discharge-initiated, pulsed HF laser as the pump source. They also observed laser oscillation on pure rotational transitions in the wavelength range 30 to 130 microns. Finally, they also reported true Dicke super-radiance on some rotational transitions in the wavelength range 50 to 250 microns. Jones and Bina[21] used the rather limited tuning of the 1.3 micron line in a Nd:YAG laser to excite the HF (2,0) overtone band to determine deactivation rates. In more recent work, a Raman-shifted Nd:YAG laser was employed by Shimoji and Djeu[22] to produce amplified spontaneous emission in HCl.

The hydrogen halide species possess strong dipole moments and since the vibrational spacings are anharmonic, overtone transitions ($v>1$) are strong. Consequently, the absorption

and emission cross sections are relatively large. The absorption and emission cross sections are perhaps the most valuable assessment tool available to evaluate the potential of a candidate laser system. They can be used to predict inversion densities and small signal gain. Often, the salient performance characteristics of an optically pumped laser can be estimated from these cross sections.

The absorption cross section is defined in Eq. (1):

$$\sigma(\nu) = (A_{ul}\lambda^2/8\pi)g(\nu)(f_u/f_l) \quad (1)$$

where λ = the wavelength of the transition,

A_{ul} is the radiative rate of the transition,

$g(\nu)$ is the lineshape factor, and

f_u/f_l is the degeneracy ratio of the two states.

The lineshape factor describes the detailed shape of the absorption or emission line. At low pressures, Doppler broadening dominates and $g(\nu)$ is described by a Gaussian, while at high pressures (typically pressures >100 Torr) the broadening is due to collisions and the lineshape is Lorentzian. While these two limiting cases are often used to describe the lineshape, in many situations, both Doppler broadening and collisional broadening are significant. Then one must use a Voigt profile that is actually a convolution of a Gaussian and a Lorentzian.

For most of the hydrogen halides, the radiative rates have been previously determined and we can accurately calculate the cross sections for both absorption and emission. In Table I we present absorption and emission cross sections calculated from published radiative rates[10] for several transitions in and HCl.

Note that for the absorption cross section we have included the relative Boltzmann population of the absorbing state in the cross section. Thus, the product of the total number

density of the hydrogen halide and the tabulated cross section is equal to the absorption coefficient, k.

Optically pumped lasers are very useful kinetic tools since selective excitation using tunable lasers allows one to form high inversion densities on time scales that are comparable to or shorter than the deactivation kinetics. Studies of the evolution of temporally and spectrally resolved laser emission can provide a wealth of information concerning energy transfer since laser oscillation often occurs not only from the particular sublevel pumped by the excitation source but also from adjacent levels that are populated by collisions. For example, in previous work on the interhalogen molecule IF, we demonstrated laser oscillation from levels that were populated via multi-level (up to five vibrational quanta) energy transfer.[5]

In this paper we present the results of a study in which HCl was optically pumped on overtone transitions (3,0) and (2,0). We observed strong and efficient laser oscillation. We also have determined a preliminary value for the self broadening coefficient of HCl on the (3,0) band by measuring the absorption width of the R_2 line as a function of HCl pressure. In addition, we developed a detailed kinetic model and comparisons are made between predicted and observed performance. These comparisons provide some insight into the extensive energy transfer processes that occur in the optically excited HCl energy manifold. Modeling of the energy transfer processes also allows calculation of optical gain coefficients as a function of time for each of the v,J levels expected to participate in the lasing process.

Description of Model

The major processes in the optically pumped HCl laser are indicated in Figure 1, which shows the relevant vibrational and rotational levels. A pulsed laser is used to prepare a

population inversion between two vibrational levels. Although the excitation laser connects only two rotational levels, as indicated in Figure 1, rapid rotational energy transfer (RET) redistributes the population among several rotational levels within the initially excited vibrational level. Depending upon the HCl pressure, this RET can compete on a kinetic time scale comparable to the pump pulse and laser build up time. Consequently, these processes must be included in any model to describe the optically pumped laser. This is significantly different from many previously demonstrated optically pumped electronic transition lasers such as the I_2 (B –> X) system.[23-25] In many electronic transition lasers, the pressure must be kept low, and as a result, much less RET occurs. The IF laser mentioned above is a notable exception[5] and behaves much like the HCl vibrational laser.

The important steps in our kinetic model are indicated in the following kinetic steps.

$$HCl(v'',J'') + h\nu_p \text{ –> } HCl(v',J') \quad (2)$$

$$HCl(v',J') + h\nu_p \text{ –> } HCl(v'',J'') + 2h\nu_p \quad (3)$$

$$HCl(v',J') + h\nu_l \text{ –> } HCl(v_f'',J_f'') + 2h\nu_l \quad (4)$$

$$HCl(v',J') \text{ –> } HCl(v_f'',J_f'') + h\nu \quad (5)$$

$$HCl(v',J') + HCl(v''=0) \text{ –> } HCl(v',J_f') + HCl(v''=0) \quad (6)$$

$$HCl(v',J') + HCl(v=0) \text{ –> } HCl(v_f',J_f') + HCl(v_f'',J_f'') \quad (7)$$

where ν_p and ν_l refer to the pump and laser emission frequencies respectively.

Equation (2) describes the optical pumping process which causes excitation of an HCl molecule from an initial level (v",J") to level (v',J'). The optical selection rules for rotational transitions in HCl are $J_f = J_i \pm 1$. While there are no strict selection rules for vibrational bands, the $\Delta v = 1$ transitions are much stronger than overtone ($\Delta v > 1$) transitions. In our experiments we focused on vibrational pump bands of v"=0 –> v'=2,3. The lasing transitions observed

included only $\Delta v=1$ transitions (e.g. v'=2 –> v"=1). We used the published radiative rates of Oba and Setser[10] for this part of the model.

Equation (3) describes stimulated emission caused by the pump laser. This term accounts for any saturation that may take place on the pump transition. Equation (5) accounts for spontaneous emission from the excited states in HCl, and Eq. (4) is the HCl laser process. Although Eqs. (4) and (5) indicate radiative emission only from the initially pumped level, the model includes many more levels and energy transfer among these levels. For example, we include vibrational levels 0 to 6 and 15 rotational levels within each of these vibrational states. Equations (6) and (7) account for vibrational and rotational energy transfer within these excited state manifolds (all rotational levels in all $v > 0$). Note that we also include rotational energy transfer within $v = 0$ in order to account for collisional redistribution within this state during the pumping pulse. This can become an important kinetic process especially at higher pressures since it tends to reduce saturation effects. For example, for strong pumping one would tend to deplete the rotational level within v" = 0 during the pump pulse. However, if rotational energy transfer is significant, population from nearby levels within v" = 0 will occur. This reduces pump saturation and permits a higher population inversion to occur.

In addition to strong lasing, important relaxation processes for HCl include: rotation-translation (R-T), and rotation-rotation (R-R), and vibration-vibration (V-V). Although Copeland et al.[14,16] have published an extensive set of rotational relaxation coefficients for all possible relaxation channels involving the levels $v = 2$, $J = 0$ through $v = 2$, $J = 6$ in HF, the data base is much less established for HCl. Consequently, we used the trends in the vibrational and rotational relaxation rates for HF as a guide for those in HCl. Indeed, for the model described here we used the HF rotational rate coefficients to describe the analogous process in HCl.

Although this is an approximation, we do not feel that this is a serious compromise since rotational energy transfer is so rapid at the pressures used in these HCl experiments. As a general statement, rotational relaxation is essentially gas kinetic and vibrational relaxation is considerably slower. Thus one expects rapid rotational redistribution in the excited vibrational level that is pumped by the pulsed excitation laser.

Vibrational relaxation in HCl has been studied by Dzelkalns and Kaufman[15] who have measured V-T,R relaxation for HF and HCl in collision with numerous gases. The model the authors used to deduce these coefficients from the data incorporated the assumption of single quantum rotational and vibrational transfer. Consequently, we modeled the relaxation process upon collision as a single quantum decrease in v and a simultaneous single quantum increase in J. An example reaction would be HCl(v = 2, J = 3) + HCl(v = 0) –> HCl(v = 1, J = 4) + HCl(v = 0). It is probable that more than one rotational level is populated in the final product distribution for any one reaction. However, since rotational equilibration (the R-T,R process) occurs on a time scale of roughly 10 ns for a typical pressure (10 Torr), the anomalous rotational state distribution created by this restriction very quickly dissipates. The much slower $\Delta v = 2$ relaxation processes were neglected.

The predictions derived from this model were compared to experimental measurements of output spectra and temporal evolutions. In addition, the output power measured was compared to model predictions. One of the goals was to verify or anchor the model with direct comparisons with experimental measurements. The HCl laser is an excellent system for such comparisons since there exists a fairly extensive data base of kinetic and spectroscopic properties. Kinetic rates for the two Cl isotopes were assumed to be equal.

For single quantum transitions, we consider four possible lasing transitions; two of which populate the v,J state from the v + 1 level, and two of which depopulate the v,J state by lasing from v to v−1. This allows cascade lasing to occur. The pairs of laser lines are due to a P and R branch being allowed for each Δv transition. These processes are described by Eqs. (8) and (9).

$$N(v+1, J+M) \rightarrow N(v,J) + h\nu \tag{8}$$

$$N(v,J) \rightarrow N(v-1, J-M) + h\nu \tag{9}$$

where M = +1 for R branch transitions and M = −1 for the P branch. The small signal gain of these transitions is given by:

$$\alpha(v+1,J,M) = \sigma(v+1,J,M)\left[N(v+1,J+M) - \frac{1+2(J+M)}{1+2J} N(v,J)\right] \tag{10}$$

and

$$\alpha(v,J-M,M) = \sigma(v,J-M,M)\left[N(v,J) - \frac{1+2J}{1+2(J-M)} N(v-1,J-M)\right] \tag{11}$$

where σ is the stimulated emission cross section. We assume a plane, non-diffracting wave to obtain the average two-way intensity for each transition. The model also explicitly accounts for broadening of the optical transition lines due to pressure broadening. A voigt profile was used and the pressure broadening coefficient measured in this work was incorporated into the model. Pressure broadening has the effect of reducing the line center absorption and emission cross section values. Consequently, as more HCl is added to the cell, the predicted absorption increases at less than a linear rate once pressure broadening becomes important. For HCl this occurs when the pressure exceeds about 20 Torr. The model also included the process of saturation on the HCl laser transition.

II. Experiment

Introduction

Two excitation pump sources were used to excite the HCl molecules: a) a Nd:YAG pumped optical parametric oscillator (OPO) provided tunable output near 1.78 µm for (2,0) excitation and b) a Raman shifted alexandrite laser was used to pump the (3,0) band near 1.18 µm. Each of these systems is described below.

OPO Pump Source

As indicated in Table I, the strongest absorption bands in the HCl (2,0) band are near 1.78 µm. For this spectral region, we used a Spectra Technologies STI Mirage 3000 OPO that provided several mJ/pulse of tunable output with a linewidth on the order of 500 MHz.

Alexandrite Laser

A Raman shifted alexandrite laser (Light Age PAL 101) was used as the source for pumping the (3,0) band near 1.2 µm. The alexandrite laser was tuned with a bi-refringent filter to 794 nm and injection seeded using a tunable, single longitudinal mode diode laser that provided tunable output in the 792 to 797 nm wavelength range. The injection seeding was facilitated using a fiber optic to couple the diode laser into the alexandrite oscillator. Fabry-Perot interferograms provided by the laser manufacturer indicated that the linewidth of the injection seeded alexandrite laser was on the order of 500 to 600 MHz.

The output of the alexandrite laser was Raman shifted using hydrogen at 350 psi. To produce the required near IR output, we used the first Stokes shift (4155 cm^{-1}). This produced approximately 20 to 25 mJ of pulsed output at in the 1190 nm region to allow pumping of individual lines in the HCl (3,0) band. For example, studies were completed pumping the R(2) line of the $H^{35}Cl$ isotope.

HCl Laser Apparatus

The apparatus used for the HCl laser experiments is indicated in Figure 2. Although there were some minor differences between the two setups for (2,0) and (3,0) pumping, the apparatus is adequately described by Figure 2. The HCl gas was contained in a 1 cm diameter stainless steel cell. Two cell lengths were used, 56 cm and 236 cm. While the 56 cm cell was used in both (2,0) and (3,0) pumping, the longer cell was used exclusively for the (3,0) excitation experiments since the absorption length for this overtone band is weaker than that for the (2,0) band. Regardless of cell length, CaF_2 windows at Brewter's angle were attached to the cell, and each cell had a CaF_2 window normal to the excitation laser beam axis. This window was used to view laser induced fluorescence with a HgCdTe detector. The optical cavities in each case used input mirrors that passed 80% of the pump beam and were 99.9% reflective at the 3.8 micron HCl laser wavelength. The HCl cavity output mirror was 20% transmissive at 3.8 microns.

As indicated in Figure 2, a long pass filter was used to separate unabsorbed pump light from the HCl laser output. A pyroelectric detector was used to measure HCl laser energy, and an InAs photodiode provided temporal profiles of the laser pulse. Spectral analysis of the HCl laser pulses was completed using a 0.3 meter McPherson monochromator (300 groove/mm, 3 µm blaze grating). A stainless steel gas handling system was used to purify the HCl via repeated

freeze/pump/thaw cycles. Pressures of HCl and any bath gases were measured with MKS Baratron capacitance manometers.

In practice, a measured pressure of HCl was loaded into the HCl cell and the excitation laser (either alexandrite laser or OPO) was scanned over an HCl absorption feature. Several sets of experiments were completed. Excitation spectra were recorded by monitoring either the total, spectrally unresolved HCl laser output or laser-induced fluorescence as a function of excitation wavelength. Initial searches for laser output were completed by filling the HCl cell with approximately 25 Torr of HCl and tuning the excitation laser through strong HCl absorption bands. Once laser oscillation was established, kinetic and spectroscopic studies were completed. These experiments included: the dependence of HCl laser output on HCl pressure, and spectroscopic and kinetic investigations.

For some experiments the HCl laser output was not spectrally dispersed and the detector monitored only broad band HCl laser output. This was a valuable diagnostic for optimizing the HCl laser. For some subsequent experiments, the HCl laser output beam was directed to the input of the McPherson 270 monochromator that was used to spectrally disperse the laser output.

III. Results

In Figure 3, we present excitation spectra resulting from pumping the (2,0) band. The two chlorine isotopes (^{35}Cl and ^{37}Cl) give rise to pairs of HCl lines as indicated in the data. Figure 4a shows spectrally resolved HCl laser spectra resulting from excitation of the R(2) line. Laser oscillation is observed from several J' levels: $J' = 2$, 3, 4, and 5. The relevant energy levels are also indicated in Figure 4b. This demonstrates the dominant role of rotational relaxation in the optically pumped $v' = 2$ level. Indeed, rotational relaxation is the fastest kinetic process

within the optically pumped level. It does not necessarily degrade the performance of the laser since many of the collisionally populated levels participate in the laser output.

In Figure 5 we show an LIF trace of the R(2) line of the (3,0) band. For these data the alexandrite laser was injection tuned by scanning the output frequency of the diode laser injection seeder. By repeating this experiment for a range of HCl pressures we observed that the absorption linewidth of the HCl varied linearly with the HCl pressure as indicated in Figure 6. From these data we estimate a self-broadening coefficient of (10 ± 1.5) MHz/Torr.

In Figure 7 we show a spectrally dispersed HCl laser output spectrum resulting from pumping the R_2 line of the (3,0) band. Several P and R branch lines are obvious, and this indicates extensive rotational relaxation prior to the onset of laser oscillation. This behavior is similar to that previously observed in HF(3,0) and (2,0).[26,27] The important point is that rotational relaxation while very rapid does not remove population from the initially pumped v level and therefore is not a significant loss mechanism.

A spectrally resolved output trace of the HC1 laser in the 236 cm cell is presented in Figure 8. The spectrum clearly shows the (3,2) and (2,1) lasing lines produced from one pass of the pump beam through the long gain cell. As expected from pumping of the R(2) (3,0) line, the P(4) (3,2) line has the most intensity. This in turn dictates that P(5) should be the strongest line in the (2,1) band, and this is evident in the spectrum. Intensity in the cascade band was observed to diminish with increasing pressure due to vibrational relaxation.

The HCl laser also was observed to be very immune to quenching by HCl. The data in Figure 9 show HCl laser relative output power on the P_3 branch of the (3,2) band as a function of HCl concentration. The laser output increases as the HCl pressure is increased to approximately 20 Torr and is then essentially flat until the pressure reaches approximately 90 Torr. This

behavior can be understood in terms of the kinetics of the optically pumped HCl laser. For example, the model described above was exercised and the results (solid line) were compared to the data in Figure 9. In the general agreement is quite good except at the lower pressures. Indeed, this suggests that the vibrational transfer rates or the self broadening coefficients used in the model need to be investigated more thoroughly.

Although the model used several hundred equations to treat the kinetic processes in the HCl energy level manifold, the overall trends in Figure 9 are due almost exclusively to the combined effects of pressure broadening of the absorption and laser transition and vibrational energy transfer that reduces the population inversion.

Often, in optically pumped lasers, there is an optimum number density of the ground state laser species with respect to output power,[1] and the data in Figure 9 emphasize this for HCl. At the low pressure end, the rather weak absorption of the HCl(3,0) band leads to a smaller population inversion. For example, the model described above predicted that 7 Torr of HCl will absorb only 7% of the pump light in a 56 cm cell. At higher pressures, larger absorptions are predicted (e.g., 28% absorption at 70 Torr), and this should result in higher inversions. However, vibrational relaxation to v=2 via HCl/HCl collisions will deplete the inversion. The self quenching rate coefficient for HCl on HCl(v=3) is $k_q=3.6 \times 10^{-12}$ cm^3 molecule^{-1} s^{-1}.[15] The kinetics code indicated that the laser threshold buildup time for HCl laser oscillation on (3,2) transitions would be about 50 ns for a variety of conditions. When the pressure of HCl is 7 Torr, the vibrational relaxation rate is only 8×10^5 s^{-1} and can be neglected with respect to laser turn on time. In contrast at 70 Torr, the vibrational relaxation rate is 8×10^6 s^{-1} and in 50 ns only 70% of the initially prepared state will remain. The predicted ratio of the expected initial inversions (during pump pulse) for these two cases is approximately four. Thus, we expect the

ratio of the output energies at 70 and 7 Torr to be approximately 4 x 0.7 = 2.8. Inspection of Figure 9 indicates qualitative agreement with these estimates.

At intermediate pressures there is a balance between absorption and quenching. In other words, as the number density is increased, the initial inversion density will be higher, but quenching will be more pronounced. At the intermediate pressures these two effects essentially "balance", and the available inversion for laser oscillation is nearly constant. At the highest pressures quenching will dominate. A similar comparison was made for (2,0) excitation, and the agreement was comparable.

We also measured the conversion efficiency of the HCl laser. For (2,0) pumping we observed an energy conversion efficiency of 30% or a 60% photon efficiency. For comparison, for (2,0) pumping the model predicted a photon efficiency of 62%. These efficiencies compare favorably with previous measurements in HF for (2,0) pumping that observed photon conversion efficiencies of greater than 50%.[26,27] The earlier results of Djeu[22] also reported high conversion efficiencies (10%) for HCl amplified spontaneous emission following excitation on the (2,0) band by a Raman shifted Nd:YAG laser[22]. Indeed, the conversion efficiencies for the optically pumped hydrogen halide lasers appear to be much greater than those for optically pumped, electronic transition diatomic lasers. This is due to the fact that in the vibrational hydrogen halide lasers, rotational energy transfer is the dominant kinetic process and it only repartitions population to neighboring rotational levels. This does not significantly reduce the laser performance since these collisionally populated levels also contribute to the laser process. In contrast, in the $I_2(B -> X)$ optically pumped laser, the efficiency is less than 1% efficient due to rapid collisional and collisionless deactivation processes such as predissociation.[23-25]

IV. Conclusions

An optically pumped HCl laser has been demonstrated using two excitation schemes: (2,0) and (3,0) pumping. For (2,0) pumping the laser was observed to be very efficient. Extensive rotational relaxation was observed within the originally pumped vibrational level. The HCl laser can be considered to be a prototype system for other hydrogen halide molecules.

Acknowledgements

Portions of this work were supported by the Air Force Phillips Laboratory, Kirtland AFB, NM and by The Chemistry and Life Sciences Directorate of The Air Force Office of Scientific Research, Washington, DC. We are very grateful for this support.

References

1. B. Wellegehausen, *IEEE J. Quant. Electron.*, QE-15, 1108 (1979).
2. J.B. Koffend, R.W. Field, D.R. Guyer, and S.R. Leone, Laser Spectroscopy III, (Springer-Verlag, New York), ed. by J.L. Hall and J.L. Carlsten, 382 (1977).
3. M.D. Burrows, S.L. Baughcum, and R. Oldenberg, *Appl. Phys. Lett.*, 46, 22, (1985).
4. S.G. Dinev and G.B. Hadjichristov, *Chem. Phys. Lett.*, 175, 216 (1990).
5. S.J. Davis, L. Hanko, and P.J. Wolf, *J. Chem. Phys.*, 82, 4831 (1985).
6. H.C. Miller and K. Yamasaki, J.E. Smedley, and S.R. Leone, *Chem. Phys. Lett.*, 181, 250 (1991).
7. V.A. Zolotarev, P.G. Kryukov, Y.P. Podmarkov, M.P. Frolov, and V.A. Shcheglov, *Sov. J. Quantum. Electron.*, 18, 643 (1988).
8. L.E. Zapata and R.J. De Young, *J. Appl. Phys.*, 54, 1686 (1983).
9. Alan B. Peterson, Curt Wittig, and Stephen R. Leone, *Appl. Phys. Lett.*, 27 , 305 (1975)
10. D. Oba, B.S. Agrawalla, and D.W. Setser, *J. Quant. Spectrosc. Radiat. Transfer*, 34, 283 (1985).
11. R.E. Meredith and F.G. Smith, "Investigations of Chemical Laser Processes, Vol II", Willow Run Laboratories, University of Michigan, Ann Arbor, MI (1971).
12. J.C. Polanyi and K.B. Woodall, *J. Chem. Phys.*, 56, 1563 (1972).
13. R.L. Wilkins and M.A. Kwok, *J. Chem. Phys*., 70, 1705 (1979).
14. R.A. Copeland, D.J. Pearson, J.M. Robinson, and F.F. Crim, *J. Chem. Phys.*, 77, 3974 (1982).
15. L.S. Dzelzkalns and F. Kaufman, *J. Chem. Phys.*, 79, 3836 (1983).

16. R.A. Copeland and F.F. Crim, *J. Chem. Phys.*, 78, 5551 (1983).

17. S.R. Leone, *J. Phys. Chem.*, Ref. Data 11, 953 (1982).

18. N. Skribanowitz, I.P. Herman, J.C. MacGillivray, and M.S. Feld, *Phys. Rev. Lett.*, 30, 309 (1973).

19. N. Skribanowitz, I.P. Herman, R.M. Osgood, Jr., M.S. Feld, and A. Javan, *Appl. Phys. Lett.*, 20, 428 (1972).

20. N. Skribanowitz, I.P. Herman, and M.S. Feld, *Appl. Phys. Lett.*, 21, 456 (1972).

21. C.R. Jones and M.J. Bina, *Appl. Phys. Lett.*, 22, 44 (1973).

22. Y. Shimoji and N. Djeu, *Appl. Phys. Lett.*, 49, 1 (1986).

23. R.L. Byer, R.L. Herbst, H. Kildal, and M.D. Levenson, *Appl. Phys. Lett.*, 20, 463 (1972).

24. J.B. Koffend and R.W. Feild, *J. Appl. Phys.*, 48, 4468 (1977).

25. J.W. Glessner and S.J. Davis, *J. Appl. Phys.*, 73, 2676 (1993).

26. S.J. Davis, W.J. Kessler, G.D. Hager, and H.C. Miller, "Lasers '92," STS Press, McLean, VA (1993).

27. H.C. Miller, D.T. Radzykewycz, G.D. Hager, W.J. Kessler, and S.J. Davis, *SPIE*, 1871, 2 (1993).

Table I. Calculated Cross Sections for Absorption and Emission for HCl.

Transition (v',v'):P or R	Wavelength (μm)	Cross Section (cm^2)
(2,0); R_2	1.73	1.0×10^{-18}
(3,0); R_2	1.18	4.9×10^{-21}
(2,1); P_2	3.8	1.6×10^{-15}
(3,2); P_2	3.8	2.1×10^{-15}

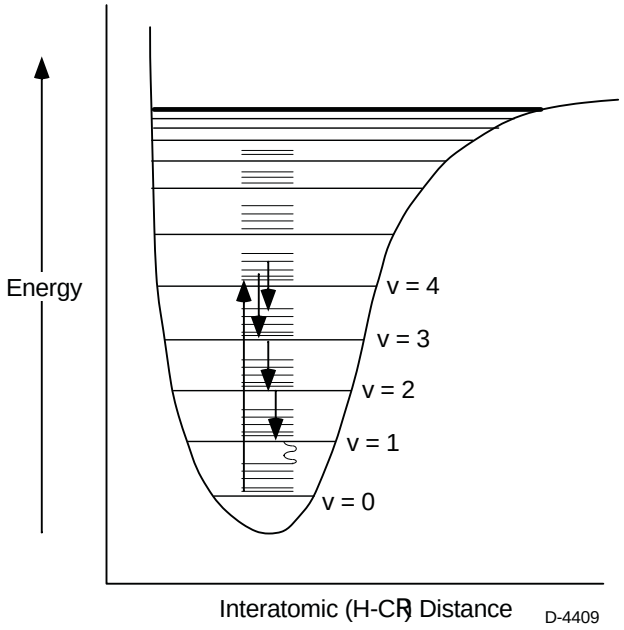

Figure 1 . Energy level diagram showing important steps in optically pumped HCl laser.

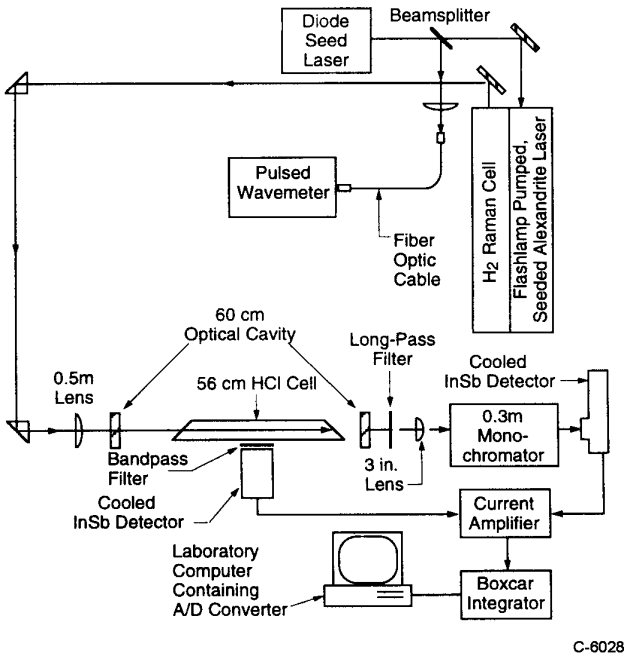

Figure 2. Block diagram of apparatus for HCl laser experiments. The Raman shifted alexandrite laser for pumping v'=3 is shown.

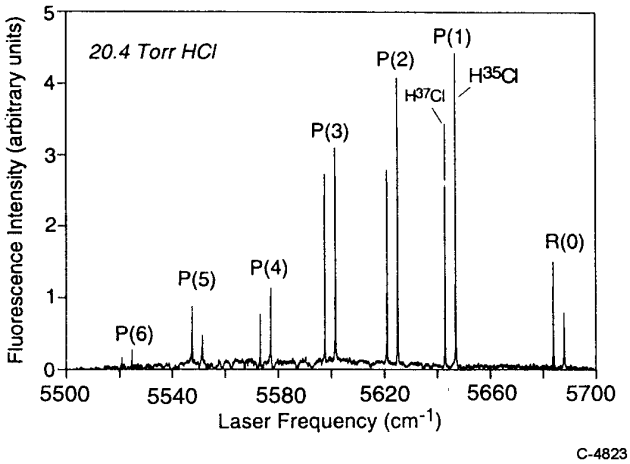

Figure 3. Laser excitation spectrum for pumping HCl (2,0) band. For these data the total spectrally unresolved HCl laser output was monitored.

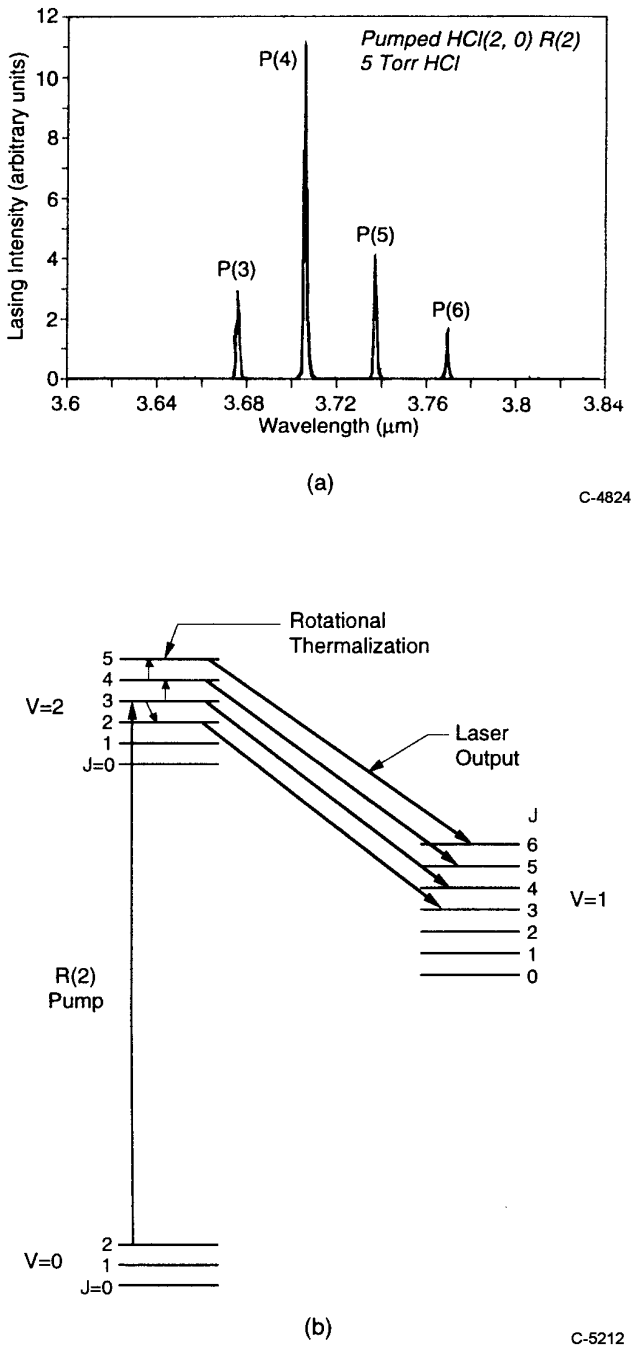

Figure 4. Spectrally resolved HCl (2,1) band laser output following pumping on the (2,0) band. Also indicated are the energy levels involved in the pump/laser process.

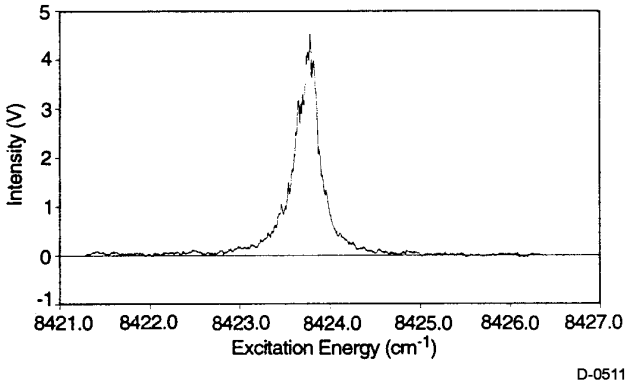

Figure 5. Laser-induced fluorescence trace of HCl R_2 line of the (3,0) band.

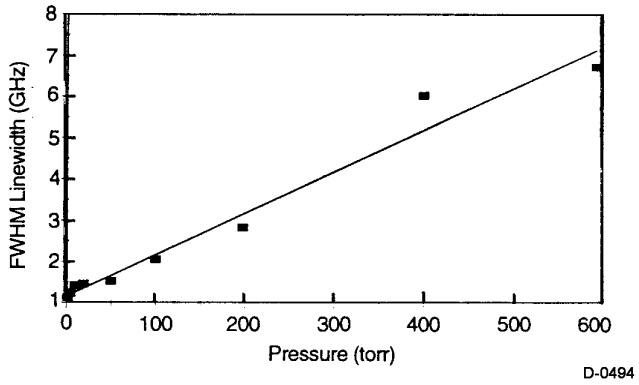

Figure 6. Plot of measured linewidth of the R(2) (3,0) HCl absorption line on as a function of HCl pressure.

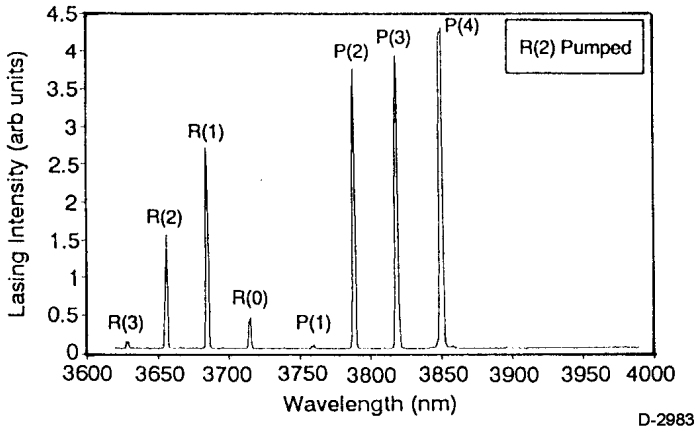

Figure 7. Spectrally resolved HCl laser output subsequent to pumping R(2) of the (3,0) band in the 56 cm gain cell with the Raman shifted alexandrite laser.

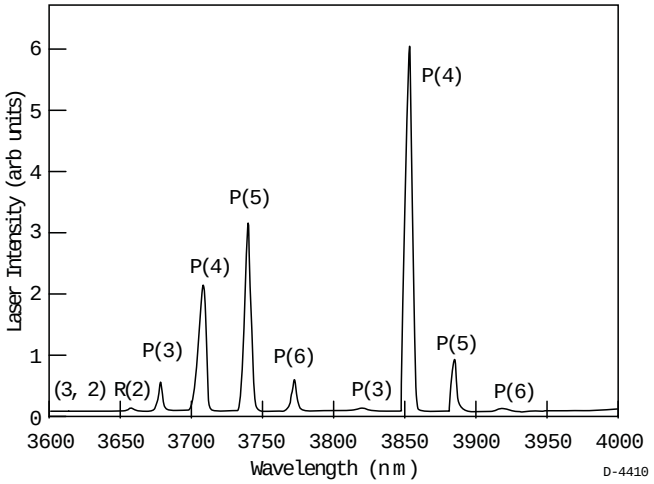

Figure 8. Spectrally resolved HC1 cascade lasing resultant from pumping R(2) of the (3,0) band in the 236 cm gain cell with the Raman shifted alexandrite laser.

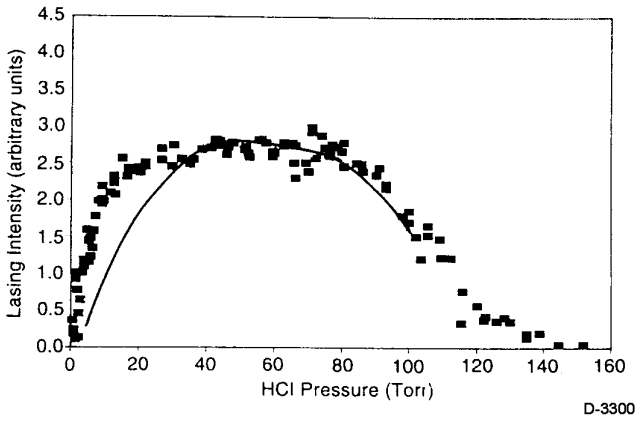

Figure 9. Dependence of HCl laser output energy (v'=3) pumping on the HCl number density. The symbols are data and the solid line represents predictions from the model.